Downloaded from http://rsta.royalsocietypublishing.org/ on February 24, 2016

PHILOSOPHICAL TRANSACTIONS A

rsta.royalsocietypublishing.org

Research

Cite this article: Zhang K, Feng XJ, Gillis K, Moldover M, Zhang JT, Lin H, Qu JF, Duan YN. 2016 Acoustic and microwave tests in a cylindrical cavity for acoustic gas thermometry at high temperature. *Phil. Trans. R. Soc. A* **374**: 20150049.
http://dx.doi.org/10.1098/rsta.2015.0049

Accepted: 23 October 2015

One contribution of 16 to a Theo Murphy meeting issue 'Towards implementing the new kelvin'.

Subject Areas:
acoustics, thermodynamics

Keywords:
cylindrical acoustic gas thermometer, waveguide, acoustic resonator, microwave resonator, thermodynamic temperature

Author for correspondence:
J.T. Zhang
e-mail: zhangjint@nim.ac.cn

Acoustic and microwave tests in a cylindrical cavity for acoustic gas thermometry at high temperature

K. Zhang[1,2], X. J. Feng[2], K. Gillis[3], M. Moldover[3], J. T. Zhang[2], H. Lin[2], J. F. Qu[2] and Y. N. Duan[2]

[1]Department of Thermal Engineering, Tsinghua University, Beijing 100084, People's Republic of China
[2]Division of Thermophysics and Process Measurements, National Institute of Metrology, Beijing 100029, People's Republic of China
[3]National Institute of Standards and Technology, Gaithersburg, MD 20899, USA

Relative primary acoustic gas thermometry (AGT) determines the ratios of thermodynamic temperatures from measured ratios of acoustic and microwave resonance frequencies in a gas-filled metal cavity on isotherms of interest. When measured in a cavity with known dimensions, the frequencies of acoustic resonances in a gas determine the speed of sound, which is a known function of the thermodynamic temperature T. Changes in the dimensions of the cavity are measured using the frequencies of the cavity's microwave resonances. We explored techniques and materials for AGT at high temperatures using a cylindrical cavity with remote acoustic transducers. We used gas-filled ducts as acoustic waveguides to transmit sound between the cavity at high temperatures and the acoustic transducers at room temperature. We measured non-degenerate acoustic modes in a cylindrical cavity in the range $295\,\mathrm{K} < T < 797\,\mathrm{K}$. The fractional uncertainty of the measured acoustic frequencies increased from 2×10^{-6} at 295 K to 5×10^{-6} at 797 K. In addition, we measured the frequencies of several transverse magnetic (TM) microwave resonances up to 1000 K in order to track changes in the cavity's length L and radius R. The fractional standard deviation of the values of L deduced from three TM modes increased from 3×10^{-6} for $T < 600\,\mathrm{K}$ to 57×10^{-6} at 1000 K. We observed similar inconsistencies in a previous study.

THE ROYAL SOCIETY PUBLISHING

© 2016 The Author(s) Published by the Royal Society. All rights reserved.

Downloaded from http://rsta.royalsocietypublishing.org/ on February 24, 2016

1. Introduction

Thermodynamic temperature T, with the SI unit of kelvin, is a measure of the average energy per degree of freedom in a system at equilibrium. Because accurate measurements of T require sophisticated techniques that are impractical in commercial applications, approximations to the kelvin scale have been developed, of which the latest are the International Temperature Scale of 1990 (ITS-90) and the Provisional Low Temperature Scale of 2000 (PLTS-2000) for $T < 1$ K. ITS-90 is an empirical scale based on a set of fixed points whose temperatures were assigned by an *a priori* determination using primary thermometry. Estimates of the difference $T - T_{90}$ have been evaluated periodically for temperatures from 0.65 to 1358 K by the Consultative Committee for Temperature (CCT). The disagreement between different measurements is still significant in the range from 25 to 273 K and from 600 to 1358 K [1]. Near the copper point (1358 K), Fischer *et al.* [1] estimated $T - T_{90}$ as (0.52 ± 0.02) K. The CCT encourages additional measurements of $T - T_{90}$ in these temperature ranges to resolve these discrepancies.

The plan to redefine the kelvin in terms of the Boltzmann constant k_B stimulated a worldwide effort to more accurately determine k_B that has advanced primary thermometry [2]. To date, acoustic gas thermometry (AGT) is the most accurate means for determining k_B. AGT determinations of k_B require absolute measurements of the speed of sound in a well-characterized monatomic gas at the temperature of the triple point of water, defined as 273.16 K [3–9]. The speed of sound is deduced from highly precise measurements of the frequencies of acoustic resonances in a monatomic gas (with a known average molar mass) confined in a cavity with known dimensions. In contrast, the ratio of resonance frequencies measured on two isotherms is a function of the ratio of the thermodynamic temperatures, but the ratio does not depend on the molar mass of the gas as long as the molar mass does not change. Likewise, the ratio will not depend on the dimensions of the cavity as long as the dimensions do not change. In reality, the dimensions of the cavity do depend on the temperature due to thermal expansion, so the ratio of acoustic resonance frequencies must be corrected by the ratios of the cavity's dimensions. The ratios of microwave resonance frequencies measured on the two isotherms are used to correct the ratio of acoustic resonance frequencies for thermal expansion [6–8]. Finally, the thermodynamic temperature of one isotherm can be determined from the corrected ratio of measured acoustic frequencies, if the other isotherm is a known fixed-point temperature. This is the basis of relative primary AGT.

Rigorous theory for waves in a cavity shows that the measured acoustic and microwave resonance frequencies must be corrected for small known perturbations to the acoustic and electromagnetic fields that occur near the cavity's walls. If the cavity expands isotropically, then the working equation for relative AGT is

$$\frac{T}{T_r} = \frac{\lim_{p\to 0} u^2(T,p)}{\lim_{p\to 0} u^2(T_r,p)} = \frac{\lim_{p\to 0}(f_a + \Delta f_a)^2/(f_m + \Delta f_m)^2}{\lim_{p\to 0}(f_a + \Delta f_a)_r^2/(f_m + \Delta f_m)_r^2}, \tag{1.1}$$

in which $u(T,p)$ denotes the speed of sound in the thermometric gas at temperature T and pressure p; f_a and f_m are the measured frequencies of acoustic and microwave resonances, respectively; Δf_a and Δf_m are corrections to the frequencies due to known perturbations; the subscript r labels a quantity measured on the reference isotherm T_r which is often at the triple point of water. Equation (1.1) relies on the ideal-gas limit, i.e. $p \to 0$. In practice, the measurements are made on isotherms as a function of p and $u^2(p,T)$ is fitted by a physically motivated function which includes the parameter $u_0^2(T)$, the value of the speed of sound at zero pressure. Equation (1.1) illustrates the principle of relative primary acoustic gas thermometers: T is determined from the measured ratios of the acoustic resonance frequencies and the microwave resonance frequencies at the unknown temperature T and at the reference temperature at T_r.

Since 1999, several laboratories have reported AGT measurements of $T - T_{90}$ spanning the range 7 to 600 K [10–16]. In the narrower range 90 K $< T <$ 384 K, data from two or more laboratories overlap; with minor exceptions, the AGT values of $(T - T_{90})/T$ are mutually

Downloaded from http://rsta.royalsocietypublishing.org/ on February 24, 2016

consistent within the fraction 3×10^{-6}. Stimulated by these impressive results, we are dealing with the technological challenges of extending the measurements of $T - T_{90}$ above 600 K [17–19].

In the moderate temperature range $90\,\mathrm{K} < T < 384\,\mathrm{K}$, our previous acoustic transducers were mounted directly in the walls of the cavity resonators. However, these transducers were constructed of materials that cannot withstand high temperatures. Instead, following Gillis *et al.* [20] and Ripple *et al.* [18], we are now using acoustic waveguides to transmit sound between the cavity at high temperature and the transducers at room temperature. Ripple *et al.* designed and explored the performance of acoustic waveguides operating from 293 to 600 K. Their novel sound source contained two identical, bending-mode, piezoelectric lead–zirconium–titanate (PZT) ceramic transducers that were driven by equal voltages at identical phase. The PZTs were mounted face-to-face on the side of the waveguide. The symmetry ensures that the vibrations of the PZTs did not move their centre of mass, thereby minimizing the coupling of the transverse motions of the PZTs to the waveguides and to the walls of the resonant cavity. The coupled PZTs also generate stronger sound pressures than a single PZT [21].

Accurately measuring the thermal expansion of the cavity resonator operating above 600 K is another technological challenge. This can be done by measuring microwave resonance frequencies [19,22–24]. Feng *et al.* [19] explored the performance of home-made antennas and microwave cables up to 1349 K. Underwood *et al.* [22,23] studied the perturbations arising from microwave probes and waveguides; they reported techniques for increasing signal-to-noise ratios and for avoiding currents at the joints between the cylindrical shell and its endplates. They used looped microwave antennas to measure both transverse electric (TE) and transverse magnetic (TM) modes. Their antennas were located at the midline of the test cavity in order to probe TE modes. They showed that the thermal expansion from 303 to 373 K determined by the TE0*pq* modes agreed with the thermal expansion determined by the TM0*pq* modes within three parts per million. The uncertainties of their measurements were only weakly dependent on temperature.

Guided by these earlier studies, we fabricated a cylindrical resonator cavity with built-in acoustic waveguides and microwave antennas. Here, we report the acoustic performance of the acoustic waveguides from 295 to 797 K and measurements of the thermal expansion of the cavity's length from 377 to 1000 K. Our objective was to test the techniques and materials at high temperatures in preparation for future thermodynamic temperature measurements.

2. Experiment set-up for high temperature

(a) Resonant frequencies in a cylindrical cavity

The acoustic resonant frequencies for non-degenerate longitudinal modes in a cylindrical cavity with length of L and radius of a are

$$f^0_{\mathrm{a},l} = \frac{ul}{2L}, \tag{2.1}$$

where u is the speed of sound and $l = 1, 2, 3\ldots$ is the longitudinal eigenvalue of the Helmholtz equation.

The microwave resonant frequencies can be represented as

$$\text{TM modes} \quad f^0_{\mathrm{TM},lmn} = \frac{c}{2\pi}\sqrt{\left(\frac{n\pi}{L}\right)^2 + \left(\frac{\chi_{lm}}{a}\right)^2} \tag{2.2}$$

and

$$\text{TE modes} \quad f^0_{\mathrm{TE},lmn} = \frac{c}{2\pi}\sqrt{\left(\frac{n\pi}{L}\right)^2 + \left(\frac{\chi'_{lm}}{a}\right)^2}, \tag{2.3}$$

where c is the speed of light in vacuum, $n = 0, 1, 2, 3\ldots$ is the longitudinal eigenvalue. For TM modes, the transverse eigenvalue χ_{lm} is the mth root of the Bessel function $J_l(x) = 0$. For TE modes, the transverse eigenvalue χ'_{lm} is the mth root of $\mathrm{d}J_l(x)/\mathrm{d}x = 0$.

The superscript 0 in equations (2.1)–(2.3) indicates that the predicted frequency is from a model that neglects perturbations, such as boundary-layer or skin-depth effects at the wall of

Downloaded from http://rsta.royalsocietypublishing.org/ on February 24, 2016

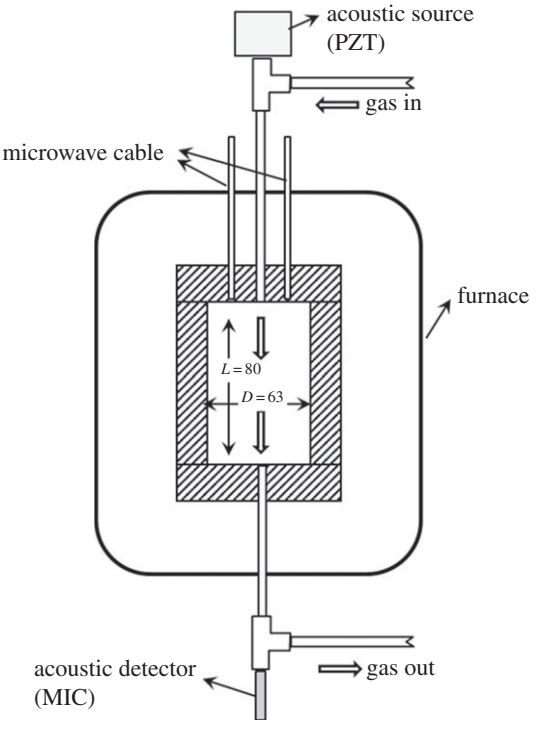


Figure 1. Schematic of the furnace, the resonator and waveguides.

the cavity, openings in the wall of the cavity and imperfect fabrication. The analyses of acoustic and microwave measurements for AGT include corrections to account for these perturbations; however, the corrections will cancel to a large degree in the ratio in equation (1.1).

(b) Experimental system

Our previous work [19] showed the successful use of the Ni–Fe–Cr alloy HR120 (Haynes International, Kokomo, IN, USA)[1] for the fabrication of the cylindrical cavity resonators with novel home-made microwave antennas and cables operating up to 1349 K. In this work, we fabricated a new cylindrical resonator that included acoustic waveguides for acoustic measurements while retaining the same, successful coaxial cables and microwave antennas that were used in [19] for thermal expansion measurements.

As illustrated in figure 1, the cavity resonator consists of a cylindrical shell with two endplates. The cylindrical shell, 80 mm long with inner diameter (ID) of 63 mm and outer diameter (OD) of 76 mm, was fabricated from a seamless HR120 tube. The endplates were 6.4 mm thick, 76 mm in diameter, and were fabricated from a HR120 plate. The endplates were welded to the ends of the cylindrical shell along the outside of the joint. The assembled resonator cavity was placed vertically in the middle of the furnace chamber. The resonator was not in a pressure vessel. The furnace chamber had an ID of 170 mm, length of 600 mm and had three independently controlled zones that provided a region 440 mm long with a temperature uniformity of ± 5 K.

Acoustic waveguides leading from the resonator to the acoustic source or detector were welded into each endplate (figure 1). Each waveguide had an ID of 4.57 mm and was made

[1]In order to describe materials and procedures adequately, it is occasionally necessary to identify commercial products by manufacturers' name or label. In no instance does such identification imply endorsement by the National Institute of Standards and Technology, nor does it imply that the particular product or equipment is necessarily the best available for the purpose.

Downloaded from http://rsta.royalsocietypublishing.org/ on February 24, 2016

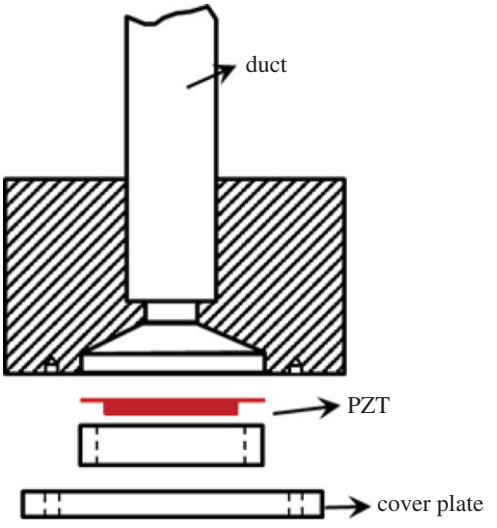


Figure 2. Source PZT transducer and housing. (Online version in colour.)

from a nickel-based high-temperature alloy GH747 (Ni 45%, Cr 16%, Al 3%, Fe balance) (CISRI, Beijing, China). The lengths of the acoustic source and detector waveguides were 340 mm and 500 mm, respectively, measured from the outer surface of the endplates to the transducers. Each waveguide was connected to a tee fitting at room temperature. The tee provided a tap for the acoustic transducers and a side port for a longer duct providing a terminal impedance that reduced acoustic reflections. The side port of the upper tee was connected to the argon supply manifold through a duct with an ID of 4.57 mm. BIP Plus argon from Air Products [25], with a claimed purity of 99.9999% was used during the tests. As we have done before [26], a getter, SAES model GC50 (SAES Pure Gas, Inc., San Luis Obispo, CA, USA), was placed downstream of the gas supply manifold for further purifying the argon before it flowed into the cylindrical cavity. The manufacturer specified that the getter reduced the mole fractions of reactive impurities to 0.05×10^{-6}. The top port of the tee fitting connected to the source transducer housing. The waveguide served two functions: it coupled sound from the source to the cavity and served as a path for flowing purified argon from the gas manifold into the cavity. We used a flow controller to maintain a flow rate of about 40 ml min^{-1}.

Figure 2 is a schematic cross section of the acoustic source assembly. The source was a single piezoelectric transducer (PZT) mounted to face the waveguide. The PZT disc had a diameter of 6 mm and a thickness of 0.5 mm and was bonded with epoxy to a 0.3 mm thick oxygen-free copper diaphragm. The electrical wires driving the source were attached directly to the surfaces of the PZT disc.

The detector waveguide (figure 1) was mounted symmetrically with respect to the source waveguide and it also was mounted on a tee fitting. Like its counterpart, the side port of the tee was connected to 4.57 mm ID tubing used to exhaust the gas from the resonator and to provide a terminal impedance to reduce reflections. The bottom port of the tee connected to the detector housing (figure 3). The detector was a 1/4 inch microphone (G.R.A.S. Sound & Vibration A/S, Holte, Denmark). The housing ensured that the pressures between the two sides of the microphone diaphragm were equal. An electrical hermetic feedthrough (LEMO) rated for operation from vacuum to 6 MPa connected the preamplifier and the power module G.R.A.S 12 AA.

The thermal expansion of the cavity's length is a key parameter for a cylindrical acoustic gas thermometer (c-AGT) operating in relative mode. Underwood & Edwards [23] measured both TE modes and TM modes using looped antennas. TE modes have significantly higher signal-to-noise

Downloaded from http://rsta.royalsocietypublishing.org/ on February 24, 2016

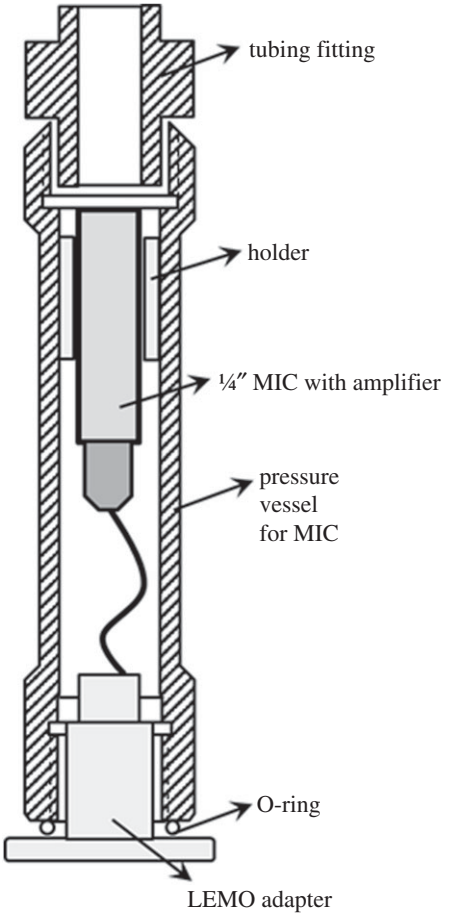


Figure 3. Microphone and housing.

ratios than TM modes. Their source and detector antennas were mounted at the midline of the cylindrical shell, separated by an angle of $\pi/2$ on the cross section perpendicular to the cylinder's axis. The TE modes generated no current at the joint between the endplate and the cylindrical cavity body. Thus, the measurements of the TE modes are anticipated to be more accurate than the TM modes. Their measurements showed that the absolute length and diameter of the cylindrical cavity determined from the TE modes differed from the length and diameter determined from the TM modes; however, the fractional changes in the length and diameter agreed within several parts per million as the temperature was changed from 313 to 373 K.

Feng *et al*. [19] designed and tested home-made coaxial cables and antennas for measuring the TM modes from 377 to 1349 K. Figure 4 shows their design. The outer conductor of each coaxial cable was a tube (3.2 mm OD; 2.2 mm ID) of Ni–Cr–Fe alloy, Inconel-625 (Special Metals Corp., Huntington, WV, USA). A line of alternating fused silica beads and fused silica tubes served as semi-flexible insulation between the outer conductor and the centre conductor. The centre conductor was a 0.5 mm diameter wire made of Ni–Cr. Each antenna was an extension of a centre conductor that protruded 1–2 mm into the cavity and coupled to the non-degenerate microwave modes TMlmn with $lmn = 010$, 011, 012, 013 and 014. Both the source and the detector antennas were embedded in one endplate of the cylindrical resonator cavity. As shown in figure 4, each antenna was insulated from the hole drilled through the endplate by a specially prepared fused silica tube. This tube had a 'bump' near one end that had been formed by a glass blower to act as a retention ring preventing the tube from sliding into the cavity. In contrast to the loop antenna

Downloaded from http://rsta.royalsocietypublishing.org/ on February 24, 2016

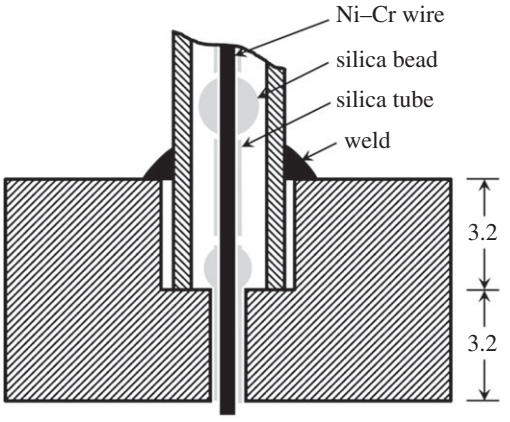


Figure 4. Antenna and feedthrough in the resonator endplate [19].

reported by Underwood & Edwards [23], we chose to use the straight wire antenna by Feng *et al*. [19] because of its simplicity and ease of assembly. See [19] for more details.

A standard S-type thermocouple (platinum/rhodium) was used to measure the temperature. This thermocouple was located approximately 3 mm from the top endplate of the cylindrical cavity. The pressure was measured with a digital pressure gauge (Druck: DPI 150).

3. Effect of waveguide at high temperature

AGTs rely on the prediction from kinetic theory that the speed of sound in a dilute gas in thermal equilibrium depends on its thermodynamic temperature. The pressure-dependence of the speed of sound is accounted for by the acoustic virial relation. AGTs accurately determine the thermodynamic temperature of a gas from measurements of the acoustic pressure response as a function of frequency near acoustic resonances in the cavity. Capacitive microphones are commonly used in AGTs because of their stability, sensitivity, and nearly flat frequency response over a wide frequency range and because they generate only small, calculable perturbations to the acoustic resonances in the cavities of typical AGTs. Additionally, PZTs have been used by the authors as both source and detector in c-AGTs. Both types of transducers have their useful temperature ranges. At temperatures above these ranges, acoustic waveguides must be used to bring sound from the source into the resonant cavity and to bring sound out of the cavity to the acoustic detector. Ripple *et al*. [18] investigated the performance of acoustic waveguides up to 600 K. Both the source and the detector were mounted in room temperature enclosures. The thermodynamic temperature measured by the AGT with the transducer–waveguide system [18] agreed well with the measurements by AGTs without such a system in the overlapping temperature range [12,15,17].

When sound propagates through a waveguide, it is attenuated by thermal and viscous dissipation in the gas and at the boundary between the gas and the walls of the waveguide. Gillis *et al*. [27] studied analytically and experimentally sound propagation inside circular, cylindrical waveguides of various lengths and diameters. Their model predicts that sound propagating inside a waveguide with radius a_d is characterized by the attenuation length l_a,

$$l_a = \frac{1}{\mathrm{Re}(\Gamma)}. \tag{3.1}$$

Here, l_a is the distance over which the amplitude of sound pressure is attenuated to 1/e of its initial value and $\mathrm{Re}(\Gamma)$ stands for the real part of Γ. The propagation parameter Γ is a complex

Downloaded from http://rsta.royalsocietypublishing.org/ on February 24, 2016

function of frequency, given by

$$\Gamma = \frac{i\omega}{u}\sqrt{\frac{1+(\gamma-1)F_t}{1-F_v}}. \tag{3.2}$$

Here, $\omega = 2\pi f$; $\gamma = C_p/C_v$, where C_p and C_v are the specific heat at constant pressure and volume, respectively. F_t and F_v are the thermal and viscous dissipation functions, respectively, which for a circular tube are given by

$$\left.\begin{aligned} F_t &\equiv \frac{2J_1(\xi_t)}{\xi_t J_0(\xi_t)}, \quad \xi_t = \frac{(1-i)a_d}{\delta_t} \\ \text{and} \qquad F_v &\equiv \frac{2J_1(\xi_v)}{\xi_v J_0(\xi_v)}, \quad \xi_v = \frac{(1-i)a_d}{\delta_v}, \end{aligned}\right\} \tag{3.3}$$

where $\delta_t = \sqrt{2\lambda/(\rho C_p \omega)}$ is the thickness of the thermal boundary layer in the gas having thermal conductivity λ and mass density ρ; and $\delta_v = \sqrt{2\eta/(\rho\omega)}$ is the thickness of the viscous boundary layer in the gas having shear viscosity η. The attenuation length increases as the duct diameter increases and decreases as the frequency increases.

When sound propagates a distance x through a duct, the acoustic pressure is attenuated by the factor e^{-x/l_a}. That is, when $x = l_a$, the sound pressure will be attenuated to 1/e of its initial pressure (assuming no reflections). Therefore the length of the waveguide between the resonator and the transducer should be no longer than approximately l_a to avoid too much attenuation [18]. On the other hand, the waveguide used for the terminal impedance (connected to the side port of tee fitting sketched in figure 1*a*) should be much longer than l_a to ensure that the sound in this waveguide is greatly attenuated to suppress resonances in the waveguide.

When resonances (standing waves) occur in the waveguide, they may couple to resonances in the cavity, thereby shifting the resonance frequencies of the cavity by an amount that is difficult to predict, and they may distort the measured frequency response profile. Standing waves occur at particular frequencies in sections of the waveguide that form quarter-wave or half-wave resonators, e.g. between the opening into the cavity and the transducer or between the transducer and the gas handling system. Standing waves in the latter section are suppressed by making the waveguide much longer than the attenuation length, as previously mentioned. Standing waves between the cavity and the transducer are suppressed by using tubes with the same ID for both sections of the waveguide and by designing the input impedance of the transducer + enclosure to be much higher than the characteristic impedance of the duct. The source and detector waveguides need not have the same ID.

The ID of the waveguide is important too. Increasing the ID increases the attenuation length, which favours larger signals at the detector, but also increases the undesirable perturbations of the cavity modes. These competing effects may be optimized. We experimentally compared the uncertainty of several resonant frequency measurements at room temperature and ambient pressure in air with a cylindrical resonator with length of 80 mm and ID of 80 mm. Table 1 compares the results of waveguides with different IDs (all the waveguide were straight, 440 mm long).

The experimental result agrees with the prediction that a waveguide with a larger ID decreases the attenuation and increases the signal-to-noise ratio, but lowers the quality factors. The waveguides with IDs of 1.75 mm and 4.57 mm represent two extreme situations. For the (200) and (500) modes, the quality factors $Q = f_r/(2g)$ of the cavity with the 4.57 mm ID were reduced to 50% and 65% of the Q with the 1.75 mm ID waveguide, respectively. The perturbations caused by the waveguides of 4.57 mm ID were significantly larger.

At elevated temperatures, the pressure was chosen to keep the density of the gas in the resonator about the same as the density at the reference temperature (so that the perturbations would be the same), but there was an unavoidable temperature gradient (and a density gradient) in the waveguide to room temperature. The presence of the gradient did not adversely affect

Downloaded from http://rsta.royalsocietypublishing.org/ on February 24, 2016

Table 1. Waveguide performance at room temperature and ambient pressure in air. The quality factor $Q = f_l/(2g)$, $\delta f_l/f_l$ is the fractional uncertainty in the fitted acoustic resonance frequency f_l, and g is the halfwidth from the fit. Note: (s) and (d) denote the source and detector waveguides, respectively.

	longitudinal mode (*l*00)							
	$l = 2$		3		4		5	
ID of waveguide (mm)	Q	$10^6\ \delta f_l/f_l$	Q	$10^6\ \delta f_l/f_l$	Q	$10^6\ \delta f_l/f_l$	Q	$10^6\ \delta f_l/f_l$
(s) 1.75	385	1.2	460	2.8	515	5.8	533	4.3
(d) 1.75								
(s) 1.75	334	1.0	416	3.1	397	2.6	475	2.8
(d) 4.57								
(s) 4.57	362	1.8	433	2.4	495	1.3	537	1.2
(d) 1.75								
(s) 4.57	192	1.8	386	1.6	372	1.5	349	1.3
(d) 4.57								

Table 2. Calculation of the perturbation to the longitudinal modes of the cylindrical cavity due to a waveguide duct at room temperature and ambient pressure in air.

	longitudinal mode (*l*00)							
	$l = 2$		3		4		5	
ID of waveguide (mm)	$10^6\ \Delta f/f$	$10^6\ g/f$	$10^6\ \Delta f/f$	$10^6\ g/f$	$10^6\ \Delta f/f$	$10^6\ g/f$	$10^6\ \Delta f/f$	$10^6\ g/f$
1.75	−12.0	94.9	−2.5	42.9	3.5	40.4	−2.7	30.0
4.57	−201.7	220.2	305.7	371.5	−130.3	173.9	121.0	183.7

the perturbations due to the waveguides because the distance over which the gradient to room temperature occurred was greater than the wavelength of sound.

Gillis *et al*. [27] developed and tested a model that predicts the shifts of the resonance frequencies of a gas-filled cavity that result when a waveguide is attached into the wall of a cavity resonator. Table 2 lists the calculated perturbations to selected resonant frequencies at room temperature and ambient pressure in air caused by the 1.75 mm ID and 4.57 mm ID waveguides. For the 1.75 mm ID waveguide, the fractional perturbations are less than or equal to 3.5×10^{-6} for the modes (300), (400) and (500); the perturbation of the (200) mode is -12.0×10^{-6}. The perturbations for the 4.57 mm ID waveguide are one order of magnitude larger.

The calculation of the waveguide-induced perturbations requires accurate values of the viscosity and thermal conductivity of the test gas. These properties are accurately known for argon and helium over a wide temperature range from recent advances in state-of-the-art measurements and from accurate, *ab initio*, quantum mechanical calculations [28–37]. We estimate that the frequency shifts caused by 1.75 mm ID waveguides can be calculated with an uncertainty of 1 ppm in the high-temperature range ($1\ \text{ppm} = 1 \times 10^{-6}$). For the sake of larger signal-to-noise ratios, we used 4.57 mm ID waveguide ducts in this first exploration of c-AGT at high temperatures.

Figure 5 shows the detected in-phase (u) and quadrature (v) acoustic signals for the (300) mode at two state points: 295 K, 201 kPa (figure 5*a*) and 797 K, 543 kPa (figure 5*b*). These pressures

Downloaded from http://rsta.royalsocietypublishing.org/ on February 24, 2016

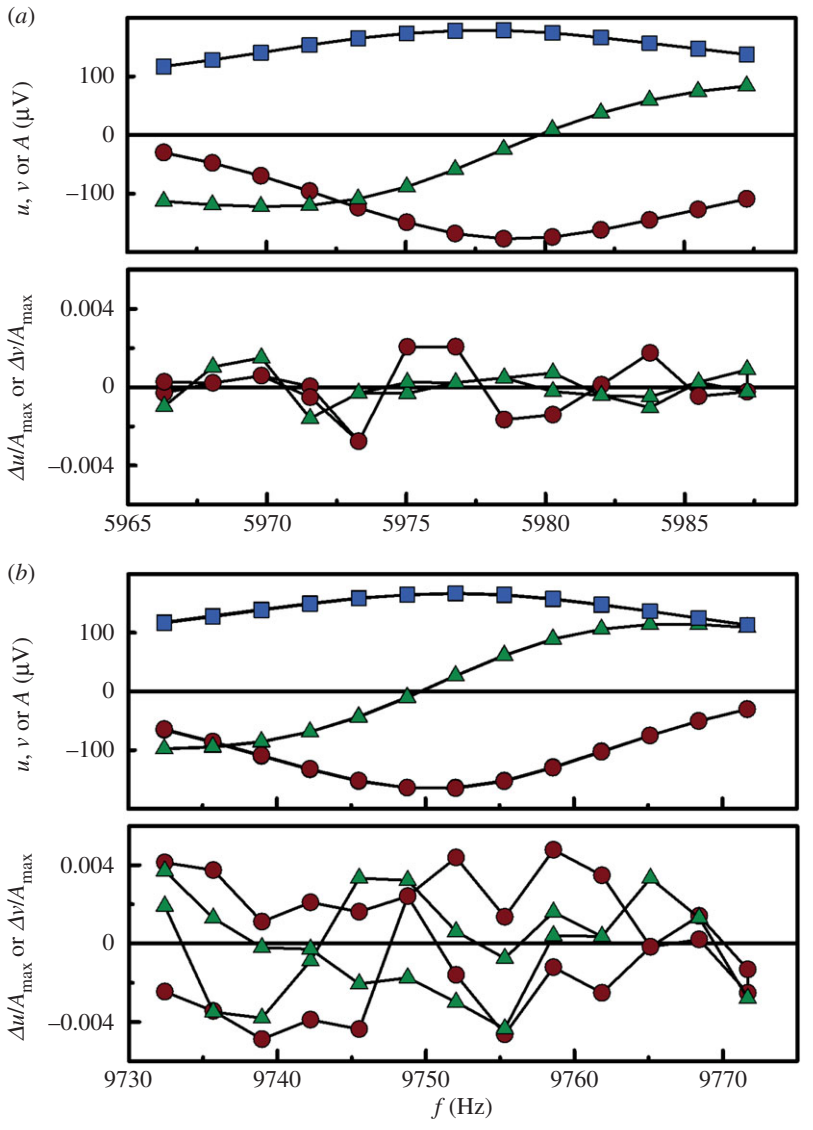


Figure 5. Comparison of measurements of the (300) acoustic mode and deviations from fits as functions of the frequency at two state points. (*a*) 295 K, 202 kPa and (*b*) 797 K, 535 kPa. The data were acquired by stepping the frequency upward and then downward through the resonance. In (*a*,*b*), the circles are the in-phase signal, triangles are the quadrature signal and squares are the amplitude. The bottom panels are the deviations from fits summarized by lines 1 and 3 in table 3. (Online version in colour.)

were chosen so that the gas densities (and the Q values) in both state points were approximately equal. The results from the fits are given in table 3. The signal-to-noise ratio at 797 K (approx. 370) is smaller than that at 295 K (approx. 870), and the deviations from fitting the resonance data at 797 K are approximately twofold larger than the deviations at 295 K. We now argue that temperature drift is responsible for some of the larger deviations from the fitted resonances at higher temperatures.

The frequency response for every resonance is measured by stepping the frequency both upward and downward through the resonance. This measurement method removes the effect of a temperature drift on the fitted resonance frequency f_r and halfwidth g to first order. During

Downloaded from http://rsta.royalsocietypublishing.org/ on February 24, 2016

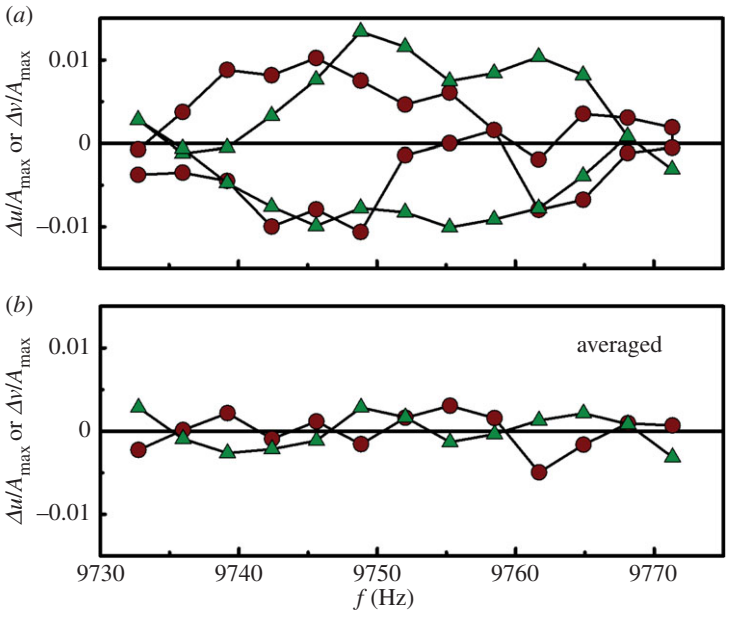


Figure 6. Comparison of fits to resonance data with a temperature drift. Deviations of the measured in-phase (circles) and quadrature (triangles) signals from two fits to data for the (300) mode at 797 K and 535 kPa, while the temperature drifted by 0.015 K. (*a*) Deviations from a fit when the up and down sweeps were not averaged first. The large systematic deviations give a poor estimate of the uncertainty in the fitted resonance frequency. (*b*) Deviations from a fit to the same data after first averaging the up and down sweeps. The fit results are listed as (a) and (b), respectively, in table 3. (Online version in colour.)

Table 3. Results from fits to measurements of mode (300) in argon. The 295 K and 797 K data in lines 1 and 3 are plotted in figure 5. During the time that the measurements labelled (a) and (b) were acquired, the temperature drifted upward by 0.015 K. (a) Inconsistency between the up and down sweeps resulted in larger deviations and higher uncertainty than (b) for which the up and down sweeps were averaged before fitting. Figure 6 compares the deviations for the two fits.

T (K)	p (kPa)	V_{pp} (V)	f_r (Hz)	g (Hz)	Q	$10^6\,\delta f/f$	$10^2\,V_{pp}Q^2\,\delta f/f$
295	202	0.3	5976.85	10.46	286	2.0	4.9
599	407	0.3	8491.61	14.52	292	2.9	7.4
797	535	0.2	9752.25	19.40	251	5.4	6.8
797 (a)	535	0.2	9753.23	19.54	250	13.0	16.3
797 (b)	535	0.2	9753.23	19.54	250	4.2	5.3

one measurement of the (300) acoustic mode at 797 K and 535 kPa, while the temperature drifted by 0.015 K. The deviations of the in-phase and quadrature signals from a fit, plotted in figure 6*a*, show inconsistencies between the up and down data that are not random and result in a large uncertainty for f_r. The fit results are labelled as (a) in table 3. When the up and down data at each frequency are averaged before fitting, the systematic effects are removed, and the deviations are much smaller and more random (figure 6*b*). Although the two fits give the same value for f_r and g, the estimated uncertainty is much smaller when these data are averaged. The right-most column in table 3 shows that the values of $\delta f/f$ at 295 and 797 K are consistent when the changes in the drive voltage and Q values of the resonances are taken into account. No unexpected problem appeared when the waveguides were subjected to the temperature gradient from 295 to 797 K.

Downloaded from http://rsta.royalsocietypublishing.org/ on February 24, 2016

Table 4. The relative thermal expansion L_T/L_0 from 377 K and the inconsistency indicated by the standard deviation of the thermal expansions obtained from three microwave modes.

T (K)	L_T/L_0	10^6 s.d.
478	1.001524	3.6
569	1.002949	2.9
673	1.004651	46.6
772	1.006368	11.8
871	1.008225	13.3
1000	1.010788	57.2

4. Thermal expansion measurement by the microwave resonant method

As sketched in figure 1, the resonator cavity has two built-in antennas used for the source and the detector of microwaves inside the cavity. Similar to Feng *et al*. [19], we used the TM010, 011, 012 and 013 modes for the measurements of the thermal expansion of the cavity length from 377 to 1000 K with flowing argon at the pressure of 200 kPa. To measure each resonance profile, we swept the frequency upward and downward in 5 MHz steps for a total of 201 points. The quality factors of the cavity modes ranged from 1600 to 2200. The signal-to-noise ratios varied from 6500 to 33 500. We calculated the radius of the cavity at each temperature from the TM010 mode, which does not depend on the cavity length. Using this radius, we obtained three measurements of the length of the cavity from the TM011, 012 and 013 modes at each temperature. Because AGT generally operates in the relative mode for measuring thermodynamic temperature, knowing the thermal expansion is necessary. The consistency among the thermal expansions extracted from the measurements of the modes is key for evaluating the microwave method. Table 4 lists the relative thermal expansion from 377 K at six temperatures and the fractional standard deviation of the thermal expansions among the modes. The measurements of the microwave frequencies were corrected from the perturbations using formulae from the literature [22,23].

The extracted thermal expansions show only small inconsistencies at 478 and 569 K, but the inconsistency increases to 57×10^{-6} at 1000 K. Except for the anomaly at 673 K, the increasing inconsistency with temperature is similar to that reported by Feng *et al*. [19], whose cavity and microwave feedthroughs were similar to the present design. The primary difference is that the new cavity is equipped with acoustic waveguides. We speculate that the anomalously large inconsistency at 673 K resulted from an undetected temperature change. Below, we will discuss the cause for the increasing standard deviation with increasing temperature.

We also measured the temperature dependence of the ratio of the cavity's length to its radius (L/a) (figure 7). Below 900 K, L/a depends linearly on temperature with a negative slope that is consistent with the linear slope observed by Feng *et al*. [19]. However, when we heated the present cavity to 1000 K, we observed an increase in the slope in figure 7 that was not reported in [19]. One difference between the present cavity and the previous cavity is the thermal history. The previous cavity had been thermally cycled between room temperature and 1350 K; the present cavity was never heated above 1000 K, where it appeared to 'age' rapidly. A certain amount of annealing may take place at elevated temperature. We will test to see if the cavity stabilizes after thermal cycling multiple times to a temperature higher than the intended range for AGT.

5. Discussion and summary

We measured the performance of the acoustic waveguides at 295 and 797 K near the argon density 82 mol m^{-3}. The deviations from the fitted resonance function at 797 K were approximately five times larger than the deviations at 295 K. By sweeping the frequency both upward and downward

Downloaded from http://rsta.royalsocietypublishing.org/ on February 24, 2016

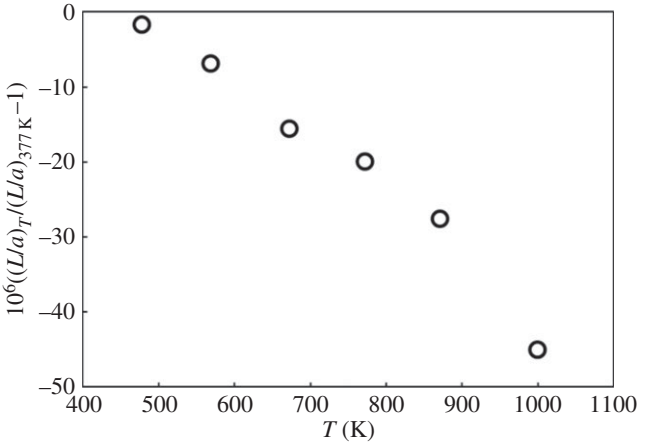


Figure 7. Temperature dependence of the ratio of the cylindrical cavity dimensions (length)/(radius) obtained from microwave measurements. Note that the vertical scale is parts per million.

to measure the resonance, we observed good reproducibility at 295 K but not at 797 K because the temperature drifted. Averaging the sweeps improves the fits, reduces the systematic deviations and lowers the estimated uncertainty of the resonance frequency. Shorter data acquisition time also reduces the effects of temperature drifts at the expense of less averaging. We plan three improvements to accurately measure $T - T_{90}$ at high temperatures. First, we will use a heat pipe inside the furnace to reduce the temperature instabilities from ±5 K to approximately ±(0.1 to 0.5) K. Second, we will place the resonator inside a pressure vessel whose temperature will be controlled on the order of a few tens of millikelvin. Third, a heater on the surface of the resonator will control the temperature of the resonator to within a few millikelvin. We also will replace the 4.57 mm ID waveguides with 1.75 mm ID waveguides.

For argon-based AGT, Moldover *et al*. [24] recommend using argon densities in the range $40\,\mathrm{mol\,m^{-3}} < \rho/M < 200\,\mathrm{mol\,m^{-3}}$, where ρ is the mass density and M is the average molar mass of the gas. In order to maintain constant ρ/M, the gas pressure must increase with increasing temperature. However, increasing the gas pressures has the undesirable effect of increasing the perturbations caused by the recoil of the solid resonator shell in response to the oscillating gas within the resonator. Previous studies [25,26] discuss perturbations from four families of normal modes of a cylindrical shell with cylindrical endplates. These include longitudinal and radial oscillations of the cylindrical body of the shell, the bending of the endplates and the recoil of the entire shell, considered as a rigid body. The frequency perturbations from the first three families of modes are predicted to have the functional form

$$\frac{(\Delta f_l)_{\mathrm{shell},i}}{f_l} \approx -(\rho u^2)_{\mathrm{gas}} \frac{G_{i,l}}{1-(f_l/f_{\mathrm{shell},i})^2}, \tag{5.1}$$

where u is the speed of sound of gas; f_l is the gas resonant frequency at the eigenvalue l; $f_{\mathrm{shell},i}$ is a resonance frequency of the shell's motion at mode index i; Δf_l is the shift of the resonant frequency f_l; $G_{i,l}$ is a compliance of the shell that depends upon the geometry and elastic properties of the shell and on the geometry of the gas mode l. The perturbations predicted by the above equation increase with gas pressure at constant density $\rho u^2 \approx (5/3)p$, where the factor (5/3) applies to monatomic gases. To counteract the undesired increase of these perturbations with temperature, we considered increasing the ratio (thickness of the shell)/(radius of cavity). However, increasing the outer dimensions of the shell or decreasing the radius of the cavity will degrade the performance of a c-AGT. Thus, a high-temperature c-AGT will rely on the general principle that perturbations from shell motions vanish linearly with the pressure at low pressures.

Downloaded from http://rsta.royalsocietypublishing.org/ on February 24, 2016

The acoustic resonance frequencies of the gas-filled cavity increase as $T^{1/2}$. For each gas mode, the frequency at 1300 K is twice the frequency at room temperature. The elastic constants of metallic cavity walls are only weakly dependent on temperature, and the frequencies $f_{\mathrm{shell},i}$ in equation (5.1) decrease only slightly with increasing temperature. Therefore, the acoustic resonances of the gas may cross some of the frequencies $f_{\mathrm{shell},i}$ as the temperature increases. Near such crossings, equation (5.1) is a poor approximation and the crossing gas mode cannot be used to determine an accurate value of T. This is one of the challenges that acoustic thermometry at temperatures up to 1350 K will encounter.

We recall that the microwave frequency ratios $(f_{\mathrm{m}} + \Delta f_{\mathrm{m}})_{p,T}/(f_{\mathrm{m}} + \Delta f_{\mathrm{m}})_{p,T_{\mathrm{ref}}}$ are not exactly equal to length ratios such as $L(p,T)/L(p,T_{\mathrm{ref}})$. When gas is admitted into a cavity at the temperature T, the microwave frequencies will decrease by the factor $1/n$, where $n(p,T)$ is the refractive index of the gas at the temperature and pressure of interest. Furthermore, the microwave frequencies will increase because the cavity shrinks under the applied hydrostatic pressure. If the walls of the cavity are made of an isotropic material with a temperature-dependent isothermal bulk modulus $B_{\mathrm{T}}(T) \equiv -V/(\partial p/\partial V)_{\mathrm{T}}$, each linear dimension shrinks by the factor $[1 + p/(3B_{\mathrm{T}})]$. If AGT is conducted at the copper point (1358 K) using argon at pressures up to 1.5 MPa, the product $\wp = n(p,T)[1 + p/(3B_{\mathrm{T}})]$ reaches a maximum value of approximately 1.0016. However, $\wp$ is very nearly a linear function of pressure. Therefore, when the pressure-dependent ratio data in equation (1.1) are fitted by a physically motivated function of the pressure that includes a term proportional to p, the temperature and pressure dependences of $\wp$ will be accounted for and the correct value of $u_0^2(T)/u_0^2(T_{\mathrm{ref}})$ will be determined. Thus, accurate AGT does not require values of the difficult-to-measure quantity $B_{\mathrm{T}}(T)$.

We used the TM modes to measure the thermal expansion of the cavity because they coupled to the cavity with the simplest, most-easily modelled antennas: straight wires. Our coaxial cables had a small diameter; therefore, they made only very small perturbations to the acoustic modes of the cavity. Our thermal expansion measurements, except for the anomaly at 673 K, agree with the results reported by Feng *et al*. [19]. Both studies indicate that the inconsistencies among the measured thermal expansions by different TM modes are at the level of 3 ppm for temperatures below 600 K; 10 ppm from 600 to 900 K; and 50 ppm at 1000 K and above. These data suggest three possible causes responsible for the phenomenon. First, the thermal expansion of the cavity may be anisotropic due to stresses in the metal from machining. If this is the case, we will use acoustic modes and TE modes with identical wavenumbers, so that the anisotropy of the thermal expansion exactly cancels out of the frequency ratios in equation (1.1). This choice completely circumvents the need to characterize the anisotropy of the thermal expansion. Second, there may be errors in the calculated corrections to the measured frequencies due to unknown current paths through the joints at the endplates. For example, a slit at this joint may open or close as the temperature changes. The sensitivity of the microwave frequency perturbations to such a slit varies from TE mode to TM mode. The effective resistance of the slit is sensitive to the slit's geometry; therefore it might explain the increasing dispersion of the TM modes with increasing temperature. We plan to eliminate this possible problem by using a new cylindrical cavity that has a single joint in the symmetry plane perpendicular to the cylinder's axis. (This joint is analogous to the joint at the 'equator' of a quasi-sphere formed by joining two quasi-hemispheres.) Third, there may be a structural change in the metal above 1000 K. The possibility can be tested by measuring the thermal expansion of the alloy using a dilatometer.

Finally, we note that thermal cycling might reduce the stress in the alloy and slow the time-dependence of the cavity's dimensions at high temperatures.

Authors' contributions. K.Z. participated in the design and the assembling of the experimental facility, carried out the major part of the experiments. X.J.F. designed the acoustic and microwave cavity for the experiments at high temperatures, directed the assembling of the facility and analysed the experimental data. K.G. originated the design of the microwave antenna and acoustic waveguide operating at high temperatures, analysed the experimental data and revised the peer-reviewed manuscript. M.M. originated the thought and the procedure for construction of acoustic and microwave resonant cavities, analysed the experimental data and edited the revision of the peer-reviewed manuscript. J.T.Z. coordinated the reported study, participated in the analysis

Downloaded from http://rsta.royalsocietypublishing.org/ on February 24, 2016

of the experimental data and drafted the manuscript. H.L., J.F.Q. and Y.N.D. participated in the design of the experiment and the analysis of the experimental data. All authors gave final approval for publication.

Competing interests. We declare we have no competing interests.

Funding. This work was supported by the National Natural Science Foundation of China (nos. 51476153, 51276175 and 61372041) and the Fundamental Research Program of NIM (no. AKY1401).

Acknowledgements. We acknowledge our great appreciations for Robin Underwood from NPL and Laurent Pitre from LNE-CNAM.

References

1. Fischer J *et al.* 2011 Present estimates of the differences between thermodynamic temperatures and the ITS-90. *Int. J. Thermophys.* **32**, 12–25. (doi:10.1007/s10765-011-0922-1)
2. White DR, Fischer J. 2015 The Boltzmann constant and the new kelvin. *Metrologia* **52**, S213–S216. (doi:10.1088/0026-1394/52/5/S213)
3. Colclough AR, Quinn TJ, Chandler TRD. 1979 An acoustic redetermination of the gas constant. *Proc. R. Soc. Lond. A* **368**, 125–139. (doi:10.1098/rspa.1979.0119)
4. Moldover MR, Trusler JPM, Edwards TJ, Mehl JB, Davis RS. 1988 Measurement of *R* using a spherical acoustic resonator. *J. Res. Natl Inst. Stand. Technol.* **93**, 85–144. (doi:10.6028/jres.093.010)
5. Fischer J. 2015 The international temperature scale and the new definition of the kelvin. In *Fundamental Constants Meeting, Eltville, Germany, 1–6 February 2015*.
6. de Podesta M, Yang I, Mark DF, Underwood R, Sutton G, Machin G. 2015 Correction of NPL-2013 estimate of the Boltzmann constant for argon isotopic composition and thermal conductivity. *Metrologia* **52**, S353–S363. (doi:10.1088/0026-1394/52/5/s353)
7. Pitre L, Risegari L, Sparasci F, Plimmer MD, Himbert ME, Giuliano Albo PA. 2015 Determination of the Boltzmann constant from the speed of sound in helium gas at the triple point of water. *Metrologia* **52**, S263–S273. (doi:10.1088/0026-1394/52/5/s263)
8. Gavioso RM, Madonna Ripa D, Steur PPM, Gaiser C, Truong D, Guianvarc'h C, Tarizzo P, Stuart FM, Dematteis R. 2015 A determination of the molar gas constant *R* by acoustic thermometry in helium. *Metrologia* **52**, S274–S304. (doi:10.1088/0026-1394/52/5/s274)
9. Feng XJ, Lin H, Gillis KA, Moldover MR, Zhang JT. 2015 Test of a virtual cylindrical acoustic resonator for determining the Boltzmann constant. *Metrologia* **52**, S343–S352. (doi:10.1088/0026-1394/52/5/s343)
10. Moldover MR, Boyes SJ, Meyer CW, Goodwin ARH. 1999 Thermodynamic temperatures of the triple points of mercury and gallium and in the interval 217 K to 303 K. *J. Res. Natl Inst. Stand. Technol.* **104**, 11–46. (doi:10.6028/jres.104.002)
11. Ewing MB, Trusler JPM. 2000 Primary acoustic thermometry between $T = 90$ K and $T = 300$ K. *J. Chem. Thermodyn.* **32**, 1229–1255. (doi:10.1006/jcht.1999.0606)
12. Strouse GF, Defibaugh DR, Moldover MR, Ripple DC. 2003 Progress in primary acoustic thermometry at NIST: 273 K to 505 K. *AIP Conf. Proc.* **684**, 31–36. (doi:10.1063/1.1627096)
13. Benedetto G, Gavioso RM, Spagnolo R, Marcarino P, Merlone A. 2004 Acoustic measurements of the thermodynamic temperature between the triple point of mercury and 380 K. *Metrologia* **41**, 74–98. (doi:10.1088/0026-1394/41/1/011)
14. Pitre L, Moldover MR, Tew WL. 2006 Acoustic thermometry: new results from 273 K to 77 K and progress towards 4 K. *Metrologia* **43**, 142–162. (doi:10.1088/0026-1394/43/1/020)
15. Ripple DC, Strouse GF, Moldover MR. 2007 Acoustic thermometry results from 271 to 552 K. *Int. J. Thermophys.* **28**, 1789–1799. (doi:10.1007/s10765-007-0255-2)
16. Underwood R, de Podesta M, Sutton G, Stanger L, Rusby R, Harris P, Morantz P, Machin G. 2016 Estimates of the difference between thermodynamic temperature and the International Temperature Scale of 1990 in the range 118 K to 303 K. *Phil. Trans. R. Soc. A* **374**, 20150048. (doi:10.1098/rsta.2015.0048)
17. Ripple DC, Defibaugh DR, Moldover MR, Strouse GF. 2003 Techniques for primary acoustic thermometry to 800 K. *AIP Conf. Proc.* **684**, 25–30. (doi:10.1063/1.1627095)
18. Ripple DC, Murdock WE, Strouse GF, Gillis KA, Moldover MR. 2013 Room temperature acoustic transducers for high-temperature thermometry. *AIP Conf. Proc.* **1552**, 44–49. (doi:10.1063/1.4819513)

Downloaded from http://rsta.royalsocietypublishing.org/ on February 24, 2016

19. Feng X, Gillis KA, Moldover MR, Mehl JB. 2013 Microwave-cavity measurements for gas thermometry up to the copper point. *Metrologia* **50**, 219–226. (doi:10.1088/0026-1394/50/3/219)
20. Gillis KA, Moldover MR, Goodwin ARH. 1991 Accurate acoustic measurements in gases under difficult conditions. *Rev. Sci. Instrum.* **62**, 2213–2217. (doi:10.1063/1.1142339)
21. Lin H, Gillis KA, Zhang JT. 2010 Characterization of piezoelectric ceramic transducer for accurate speed-of-sound measurement. *Int. J. Thermophys.* **31**, 1234–1247. (doi:10.1007/s10765-010-0795-8)
22. Underwood RJ, Mehl JB, Pitre L, Edwards G, Sutton G, de Podesta M. 2010 Waveguide effects on quasispherical microwave cavity resonators. *Meas. Sci. Technol.* **21**, 075103. (doi:10.1088/0957-0233/21/7/075103)
23. Underwood RJ, Edwards GJ. 2014 Microwave-dimensional measurements of cylindrical resonators for primary acoustic thermometry. *Int. J. Thermophys.* **35**, 971–984. (doi:10.1007/s10765-014-1726-x)
24. Moldover MR, Gavioso RM, Mehl JB, Pitre L, de Podesta M, Zhang JT. 2014 Acoustic gas thermometry. *Metrologia* **51**, R1–R19. (doi:10.1088/0026-1394/51/1/r1)
25. Zhang JT, Lin H, Feng XJ, Sun JP, Gillis KA, Moldover MR, Duan YY. 2011 Progress toward redetermining the Boltzmann constant with a fixed-path-length cylindrical resonator. *Int. J. Thermophys.* **32**, 1297–1329. (doi:10.1007/s10765-011-1001-3)
26. Lin H, Feng X, Gillis K, Moldover M, Zhang J, Sun J, Duan Y. 2013 Improved determination of the Boltzmann constant using a single, fixed-length cylindrical cavity. *Metrologia* **50**, 417–432. (doi:10.1088/0026-1394/50/5/417)
27. Gillis K, Lin H, Moldover M. 2009 Perturbations from ducts on the modes of acoustic thermometers. *J. Res. Natl Inst. Stand. Technol.* **114**, 263–285. (doi:10.6028/jres.114.019)
28. Berg RF. 2005 Simple flow meter and viscometer of high accuracy for gases. *Metrologia* **42**, 11–23. (doi:10.1088/0026-1394/42/1/002)
29. May EF, Moldover MR, Berg RF, Hurly JJ. 2006 Transport properties of argon at zero density from viscosity-ratio measurements. *Metrologia* **43**, 247–258. (doi:10.1088/0026-1394/43/3/007)
30. May EF, Berg RF, Moldover MR. 2007 Reference viscosities of H_2, CH_4, Ar, and Xe at low densities. *Int. J. Thermophys.* **28**, 1085–1110. (doi:10.1007/s10765-007-0198-7)
31. Vogel E, Jäger B, Hellmann R, Bich E. 2010 *Ab initio* pair potential energy curve for the argon atom pair and thermophysical properties for the dilute argon gas. II. Thermophysical properties for low-density argon. *Mol. Phys.* **108**, 3335–3352. (doi:10.1080/00268976.2010.507557)
32. Vogel E. 2010 Reference viscosity of argon at low density in the temperature range from 290 K to 680 K. *Int. J. Thermophys.* **31**, 447–461. (doi:10.1007/s10765-010-0760-6)
33. Cencek W, Przybytek M, Komasa J, Mehl JB, Jeziorski B, Szalewicz K. 2012 Effects of adiabatic, relativistic, and quantum electrodynamics interactions on the pair potential and thermophysical properties of helium. *J. Chem. Phys.* **136**, 224303. (doi:10.1063/1.4712218)
34. Mehl JB. 2009 Ab initio properties of gaseous helium. *C. R. Phys.* **10**, 859–865. (doi:10.1016/j.crhy.2009.10.009)
35. Berg RF, Moldover MR. 2012 Recommended viscosities of 11 dilute gases at 25°C. *J. Phys. Chem. Ref. Data* **41**, 043104. (doi:10.1063/1.4765368)
36. Zhang JT, Lin H, Che J. 2013 Effects of connecting tubing on a two-capillary viscometer. *Metrologia* **50**, 377–384. (doi:10.1088/0026-1394/50/4/377)
37. Lin H, Feng XJ, Zhang JT, Liu C. 2014 Using a two-capillary viscometer with preheating to measure the viscosity of dilute argon from 298.15 K to 653.15 K. *J. Chem. Phys.* **141**, 234311. (doi:10.1063/1.4903960)